





























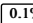
8.4%


Not yet Date: 2022-02-14 05:19 UTC


* All sources 100 | Internet sources 37 | Publisher sources 5 | Organization archive 5 | Plagiarism Prevention Pool 39


- [0] www.researchgate.net/publication/324170859_A_review_of_the_hydrothermal_carbonization_of_biomass_waste_for_hydrochar_formation_Process
3.4% 62 matches
- [1] www.researchgate.net/publication/265169649_Effects_of_wet_torrefaction_on_reactivity_and_kinetics_of_wood_under_air_combustion_conditions
2.1% 65 matches
- [2] pubs.acs.org/doi/10.1021/acsomega.1c01787
1.6% 43 matches
- [4] curve.carleton.ca/system/files/etd/f2dce676-3e4d-41dd-9675-0a8cc1d6b8e4/etd_pdf/1b2b71f95e50de45befa7f96822aeb9a/ghaziaskar-catalysedhydr
1.9% 43 matches
- [6] www.researchgate.net/publication/51533579_Hydrothermal_carbonization_of_anaerobically_digested_maize_silage
1.1% 26 matches
- [9] link.springer.com/article/10.1007/s12649-020-01255-3
0.4% 36 matches
- [10] ietresearch.onlinelibrary.wiley.com/doi/full/10.1049/rpg2.12082
0.9% 28 matches
- [11] from a PlagScan document dated 2017-10-26 05:26
0.1% 40 matches
- [12] www.researchgate.net/publication/327322513_Hydrothermal_Carbonization_of_Biosolids_from_Waste_Water_Treatment_Plant
0.5% 30 matches
- [13] from a PlagScan document dated 2021-07-21 07:13
0.6% 29 matches
- [14] Hydrothermal treatment of banana leaves for solid fuel combustion
0.1% 33 matches
- [15] www.mdpi.com/1996-1073/13/16/4164/htm
0.2% 31 matches
- [16] www.nature.com/articles/s41598-020-75936-3
0.8% 28 matches
- [17] www.ncbi.nlm.nih.gov/pmc/articles/PMC7606520/
0.8% 28 matches
- [18] hull-repository.worktribe.com/OutputFile/798417
0.9% 21 matches
- [19] www.mdpi.com/1996-1073/13/16/4164/pdf
0.1% 28 matches
- [20] from a PlagScan document dated 2017-09-08 16:40
0.7% 18 matches
- [21] www.researchgate.net/publication/324977049_Hydrothermal_carbonization_as_an_all-inclusive_process_for_food-waste_conversion
0.2% 29 matches
- [22] www.jeijc.org/wp-content/uploads/2021/03/unep21-food-waste-index-report-2021.pdf
0.6% 20 matches
- [23] www.researchgate.net/publication/333160242_Gasification_and_Properties_of_Chars_Derived_Food_Waste_by_Pyrolytic_and_Hydrothermal_Carb
0.5% 25 matches
- [24] link.springer.com/article/10.1007/s13399-020-00771-5
0.5% 22 matches
- [25] from a PlagScan document dated 2018-09-08 15:41
0.2% 25 matches
- [26] from a PlagScan document dated 2017-12-10 21:54
0.3% 22 matches
- [27] from a PlagScan document dated 2019-02-03 02:19
0.2% 24 matches
1 documents with identical matches
- link.springer.com/content/pdf/10.1007/s40090-016-0081-0.pdf


- [29]  link.springer.com/content/pdf/10.1007/s10059-010-0001-0.pdf
0.5% 23 matches
-
- [30]  Combustion characteristics and kinetics study of hydrothermally treated paper sludge by thermogravimetric analysis
0.2% 26 matches
-
- [31]  from a PlagScan document dated 2018-12-17 14:31
0.4% 20 matches
-
- [32]  www.researchgate.net/publication/291424494_Preparation_and_characterization_of_hydrochar_from_waste_eucalyptus_bark_by_hydrothermal_car
0.7% 16 matches
-
- [33]  www.researchgate.net/publication/326649192_EVALUATION_OF_UTILISING_INGELIA_HYDROCHAR_PRODUCED_FROM_ORGANIC_RE
0.3% 22 matches
-
- [34]  from a PlagScan document dated 2020-04-03 21:28
0.5% 17 matches
-
- [35]  from a PlagScan document dated 2018-11-12 09:16
0.1% 24 matches
-
- [36]  www.mdpi.com/1996-1073/11/8/2022/pdf
0.4% 19 matches
-
- [37]  from a PlagScan document dated 2018-06-11 21:11
0.1% 25 matches
-
- [38]  bioresourcesbioprocessing.springeropen.com/articles/10.1186/s40643-020-00350-6
0.4% 17 matches
-
- [39]  from a PlagScan document dated 2015-12-01 11:13
0.1% 22 matches
-
- [40]  www.ncbi.nlm.nih.gov/pmc/articles/PMC6227982/
0.3% 20 matches
-
- [41]  Effect of Equivalence Ratio and Particle Size on EFB Char Gasification
0.1% 22 matches
-
- [42]  from a PlagScan document dated 2019-08-06 12:40
0.1% 20 matches
-
- [43]  from a PlagScan document dated 2019-07-25 12:32
0.1% 19 matches
-
- [44]  from a PlagScan document dated 2019-11-26 13:27
0.3% 19 matches
-
- [45]  from a PlagScan document dated 2017-12-07 21:34
0.3% 14 matches
-
- [46]  bioresources.cnr.ncsu.edu/resources/effect-of-temperature-on-the-properties-of-charcoal-prepared-from-carbonization-of-biorefinery-lignin/
0.2% 16 matches
-
- [47]  "Synthesis of chemically modified BisGMA analog with low viscosity and potential physical and biological properties for d.pdf" dated 2019-11-06
0.1% 18 matches
-
- [48]  core.ac.uk/download/pdf/84073897.pdf
0.1% 13 matches
-
- [50]  www.mdpi.com/1996-1073/12/5/858/pdf
0.2% 15 matches
-
- [51]  from a PlagScan document dated 2020-05-21 22:27
0.1% 14 matches
-
- [52]  from a PlagScan document dated 2017-03-26 13:52
0.1% 13 matches
-
- [53]  www.researchgate.net/profile/Nizamuddin_Sabzoi2/publication/324030318_Upgradation_of_chemical_fuel_thermal_and_structural_properties_of_r
0.3% 12 matches
-
- [54]  Laboratory-scale Pyrolysis of Oil Palm Trunks
0.0% 15 matches
-
- [55]  www.researchgate.net/publication/230463259_Competition_Between_Hydrotreating_and_Polymerization_Reactions_During_Pyrolysis_Oil_Hydrod
0.2% 12 matches
-
- [56]  "21947.pdf" dated 2017-10-30
0.1% 14 matches
-
- [57]  "Manuscript-(19-03-2019).docx" dated 2019-03-19


- []  0.1% 12 matches


- [59]  from a PlagScan document dated 2016-11-23 12:41
 0.0% 15 matches


- [60]  from a PlagScan document dated 2015-11-29 08:39
 0.0% 17 matches


- [61]  from a PlagScan document dated 2020-06-15 12:42
 0.1% 13 matches


- [62]  from a PlagScan document dated 2018-02-12 07:25
 0.0% 14 matches


- [63]  from a PlagScan document dated 2018-06-25 09:55
 0.2% 10 matches


- [64]  from a PlagScan document dated 2020-08-03 13:42
 0.0% 14 matches


- [65]  from a PlagScan document dated 2017-09-16 16:18
 0.1% 12 matches


- [66]  Physicochemical characteristics and pyrolysis kinetics of raw and torrefied hybrid poplar wood (NM6 – Populus nigra)
 0.0% 14 matches


- [67]  from a PlagScan document dated 2020-02-24 19:41
 0.3% 9 matches

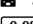
- [68]  from a PlagScan document dated 2020-05-29 17:03
 0.1% 12 matches

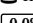
- [69]  from a PlagScan document dated 2020-05-14 09:58
 0.1% 11 matches

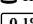
- [70]  www.hindawi.com/journals/isrn/2013/268947/
 0.0% 12 matches

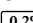
- [71]  digital.csic.es/bitstream/10261/259112/1/innowaste.pdf
 0.1% 10 matches

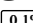
- [72]  from a PlagScan document dated 2018-10-04 08:24
 0.0% 13 matches

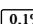
- [73]  "77.pdf" dated 2020-12-14
 0.0% 13 matches

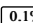
- [74]  from a PlagScan document dated 2018-08-15 11:05
 0.0% 10 matches

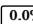
- [75]  from a PlagScan document dated 2018-03-06 20:39
 0.1% 10 matches

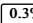
- [76]  www.researchgate.net/publication/349324184_Insights_on_Molecular_Characteristics_of_Hydrochars_by_13_C-NMR_and_Off-Line_TMAH-GCMC
 0.2% 9 matches

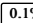
- [77]  from a PlagScan document dated 2017-09-11 17:19
 0.1% 8 matches

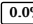
- [78]  from a PlagScan document dated 2017-08-17 10:55
 0.1% 11 matches

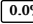
- [79]  www.researchgate.net/figure/Ultimate-analysis-ash-and-lignin-number-for-all-raw-and-hydrochar-samples-a-indicates_tbl3_331540007
 0.1% 10 matches


- [81]  from a PlagScan document dated 2020-12-21 12:35
 0.0% 13 matches

- [82]  www.researchgate.net/figure/Mass-yield-energy-yield-and-energy-densification-ratio_tbl1_326824024
 0.3% 8 matches


- [83]  from a PlagScan document dated 2019-03-19 09:49
 0.1% 12 matches


- [84]  www.researchgate.net/publication/318372688_Evaluating_the_Potential_Impact_of_Hydrochar_on_the_Production_of_Short-Chain_Fatty_Acid_fr
 0.0% 9 matches



- [86]  from a PlagScan document dated 2021-11-04 13:38
 0.0% 11 matches


- [87]  from a PlagScan document dated 2021-09-20 07:53

0.0% 11 matches


[89]  from a PlagScan document dated 2019-06-23 09:34
0.0% 9 matches


[91]  www.researchgate.net/publication/347856997_Evaluation_of_the_Potential_of_Agricultural_Waste_Recovery_Energy_Densification_as_a_Factor_f
0.0% 9 matches

[92]  "Revised Manuscript-JNN_2019_0106.docx" dated 2019-10-23
0.1% 7 matches
 2 documents with identical matches

[95]  www.researchgate.net/figure/Energy-yield-and-energy-densification-ratio-of-hydrothermal-carbonization-experiments-as_fig3_342068505
0.0% 11 matches

[96]  www.mdpi.com/2306-5729/5/2/48/htm
0.2% 7 matches

[98]  from a PlagScan document dated 2018-01-15 10:25
0.1% 7 matches

[102]  from a PlagScan document dated 2021-04-12 08:27
0.0% 9 matches

22 pages, 6622 words

PlagLevel: 8.4% selected / 19.6% overall

214 matches from 104 sources, of which 39 are online sources.

Settings

Data policy: *Compare with web sources, Check against organization repository, Check against the Plagiarism Prevention Pool*

Sensitivity: *High*

Bibliography: *Bibliography excluded*

Citation detection: *Highlighting only*

Whitelist: --

1 Physicochemical properties and combustion kinetics of food waste derived
2 hydrochars

3 Moonis Ali Khan^{a,*}, B. H. Hameed^b, Masoom Raza Siddiqui^a, Zeid A. Alothman^a, Ibrahim H
4 Alsohaimi^c

5 ^aChemistry Department, College of Science, King Saud University,
6 Riyadh 11451, Saudi Arabia

7 ^bDepartment of Chemical Engineering, College of Engineering, Qatar University,
8 P.O. Box: 2713, Doha, Qatar

9 ^cChemistry Department, College of Science, Jouf University, Sakaka, Saudi Arabia
10

11

12

13

14

15

16

17 Keywords: Food waste, Hydrothermal carbonization, Hydrochar, Thermogravimetric
18 analysis, Kinetics

19

20

21

22

23 Abstract

24 In this work, simulated food waste (15 % white bread, 15% palm dates (without seeds), 5%
25 boiled egg (without shells), 20% spent tea leaves, 20% spent coffee ground, and 25% banana
26 peel in parts weight) was subjected to hydrothermal carbonization (HTC) at 180, 200 and 220
27 °C for 120 min.^[6] The mass yield and energy yield of the resultant hydrochars viz. HTC180,
28 HTC200, and HTC220 were 69.46, 68.50, 65.35 % and 88.91, 87.68, 84.30%, respectively.
29 Among the hydrochars produced, HTC220 had the highest heating value (HHV: 23.61
30 MJ/kg), while the food waste had a HHV of 18.17 MJ/kg.^[2] Activation energy for the
31 combustion of food waste and HTC220 was determined by modelling the thermogravimetric
32 data using the Arrhenius equation and was found to be in the range of 29.98 to 33.51 kJ/mol
33 and 16.52 to 25.47 kJ/mol, respectively. The densification ratio for the three hydrochar
34 samples varied slightly (1.28-1.29).^[6] The results indicate that the hydrochar produced from
35 food waste could be a potential to substitute coal combustion.

36

37

38

39

40

41

42

43

44 *Corresponding Author: Moonis Ali Khan

45 E-mail addresses: mokhan@ksu.edu.sa; moonisalikhan@gmail.com

46 1. Introduction

47 Food waste is documented as one of the challenges confronting the world today with severe
48 impacts on the environment. ^[22] The Food Waste Index Report, 2021 recently released from the
49 United Nations Environment Programme (UNEP) indicated that roughly 0.93 billion tonnes
50 of food was discarded as waste in 2019 (UNEP, 2021). ^[22] The 2015 United Nations sustainable
51 development agenda identified food waste as a core challenge to be addressed in order to
52 achieve sustainable consumption. The agenda outlined in section 12.3 and 12.5 of Sustainable
53 Development Goal for cutting in half per capita global food waste and significantly
54 minimizing waste generation respectively necessitates a sustainable approach for complete
55 waste valorisation besides mitigation strategies (Ishangulyyev et al., 2019).

56 Religious pilgrimages are one of the major global food waste generators. For instance,
57 annually, around 10 million pilgrims from all over the world travel to the Kingdom of Saudi
58 Arabia (KSA) for Hajj and Umrah pilgrimages. Trend shows a steady increase in Hajj
59 pilgrims from 5.6 million in 2015 to 7.4 million in 2019 (Atique and Itumalla, 2020). ^[20] The rise
60 in the number of pilgrims and donation of packed and unpacked food during Hajj and Umrah
61 continue to increase, consequently generating large amount of food waste. ^[20] A nationwide field
62 study estimated that the amount of food waste generated annually in KSA is about 427 kg per
63 person (Baig et al., 2019).

64 Although, increasing amount of food discarded as waste during Hajj pilgrimage puts
65 significant burden on the environment, it is an unexploited opportunity. Food waste is
66 chemically composed of varied organic compounds which are classified into carbohydrates,
67 proteins and lipids (Alibardi and Cossu, 2016). This makes food waste suitable to be
68 processed into a stable and nutrient-rich organic fertilizer, hydrochar, and value-added
69 chemicals. The physicochemical characteristics of food waste hydrochar obtained by

70 hydrothermal carbonization (HTC) have an elemental carbon composition and heat content
71 up to 73% and 31 MJ/kg, respectively (Saqib et al., 2018).

72 Therefore, re-utilising food waste through chemical conversion processes is essential
73 for sustainable environmental development. The conventional food waste conversion
74 technologies includes torrefaction (Singh and Yadav, 2019), co-hydrothermal carbonization
75 (Alshareef et al., 2022), pyrolysis (Cao et al., 2019), and fermentation (Carmona-Cabello et
76 al., 2020). Another conventional but recently revived technology is HTC process. This
77 process is flexible and easily adaptable for wide range of applications.

78 Generally, the food waste stream of municipal solid waste in KSA contains
79 approximately 38.4% moisture with low heating values (Nizami et al., 2017), which makes
80 its incineration to be energetically inefficient.^{[0]▶} Compared to pyrolysis, HTC is conducted at
81 moderate temperature and can efficiently convert wet and heterogeneous food waste into
82 highly dense hydrochar, resembling coal in terms of its physical and chemical properties (Li
83 et al., 2013). Yan et al., (2022) carried out the HTC of kitchen food waste mixture at various
84 temperatures ranging between 200 and 300 °C to produce hydrochars. The HHV of the
85 hydrochar significantly improved from 16.4 MJ/kg to 18.33 - 20.6 MJ/kg, which was
86 comparable with 20 MJ/kg, specified for coal in the literature (Al-Aboosi et al., 2021).^{[9]▶}
87 Additionally, HTC of the food waste mixture produced a hydrochar with an improved
88 physical and chemical properties compared to hydrochar derived from the HTC of the
89 individual component of the feedstock mixture.

90 Thus, HTC is a sustainable and eco-friendly tool for converting KSA food waste into
91 value-added products like catalyst (Abdullah et al., 2021) and adsorbents (Ashareef et al.,
92 2021). In this study, hydrochars were produced from simulated food waste (similar to Hajj
93 and Umrah food waste) through HTC process route. The physicochemical properties and
94 combustion kinetics of the simulated food waste and produced hydrochars were determined.

95 2. Materials and methods

96 2.1. Materials

97 Locally consumed food waste such as white bread, palm date, egg, banana, spent coffee, and
98 tea were collected, oven dried for a week at 60 °C, crushed and sieved to the desired particle
99 size (0.50-1.00 mm). Thereafter, the food samples were mixed as follows: 15 % white bread,
100 15% palm dates (without seeds), 5% boiled eggs (without shells), 20% spent tea leaves, 20%
101 spent coffee ground, and 25% banana peel in parts weight.

102 2.2. Preparation of hydrochar

103 10 g of the food waste feedstock sample was placed inside an automated hydrothermal vessel
104 (170 mL). 90 mL of deionized (D.I) water was added to it and mixed to obtain a feedstock to
105 water ratio of 10% w/w. The submerged sample was agitated at room temperature for 30 min.
106 Thereafter, the contents inside the reactor vessel were heated at 180 °C for 120 min under
107 5 °C/min heating rate. Finally, the vessel was instantly cooled to ambient temperature with
108 the help of cooling jacket around the vessel. The content was vacuum filtered with a filter
109 paper (0.45 µm) and unwanted soluble species were rinsed out by D.I water. The recovered
110 hydrochar were subsequently oven-dried at 60°C till when there was no longer change in
111 mass, indicating complete dryness. Similar procedure was repeated to produce hydrochar
112 samples at 200 and 220 °C. The dried hydrochar samples produced at 180, 200, and 220 °C
113 were code named as HTC180, HTC200, and HTC220, respectively.

114 ^[4] 2.3. Characterization of feedstock and hydrochar

115 Mass yield, energy densification ratio, and energy yield of the produced hydrochars were
116 determined according to Eqs. 1-3:

117
$$\text{Mass yield} = \frac{\text{mass of dried hydrochar}}{\text{mass of dried raw material}} \times 100 \quad (1)$$

118
$$\text{Energy densification ratio} = \frac{\text{HHV of hydrochar}}{\text{HHV of raw material}} \quad (2)$$

119 Energy yield = mass yield x energy densification ratio (3)

120 Scanning electron microscope (SEM: ^[32]Hitachi, TM3030Plus, Tabletop Microscope,
121 Japan) at a magnification of 500× was used to examine the microstructure as well as the
122 surface morphology of the food waste and derived hydrochars. Prior to SEM examination,
123 dried samples were first gold-coated in order to obtain high-resolution images. The sample
124 surface functional groups were ascertained using a Fourier transmission infrared
125 spectrophotometer (FT-IR: Perkin- Elmer, Spectrum RXI, USA) in the range between 4000-
126 500 cm⁻¹.

127 The proximate analysis was carried out using thermogravimetric analysis (TGA:
128 Perkin Elmer). The elemental analysis (CHNSO) for the feedstock and the produced
129 hydrochars were obtained using the elemental analyser (Elementar, Analysensysteme GmbH,
130 Model: VARIO EL III).

131 2.4. Combustion kinetic analysis of food waste and hydrochar

132 Combustion kinetics of food waste and hydrochar was investigated using Simultaneous
133 Thermal Analyzer –STA 449 F5 Jupiter, Germany. The sample (10 ± 0.5 mg) ^[41] was heated
134 from 50 to 900 °C under oxygen environment at heating rate of 10 °C/min. ^[1] The derivation for
135 the combustion kinetic model using the Arrhenius approach that was used for the
136 determination of the kinetic parameters in this work can be found elsewhere (Sait et al., 2012)
137 and the final equation can be expressed as

$$138 \ln \left[-\frac{\ln(1-\alpha)}{T^2} \right] = \ln \left[\frac{AR}{\beta E} \right] - \frac{E}{R} \left(\frac{1}{T} \right) \quad (4)$$

139 From Eq. 4, the graph of $\ln \left[-\frac{1-(1-\alpha)}{T^2(1-n)} \right]$ against $\frac{1}{T}$ and $\ln \left[-\frac{\ln(1-\alpha)}{T^2} \right]$ against $\frac{1}{T}$ was plotted.

140 The slope and intercept of the linearized graph should be $-E/R$ and $\ln[AR/\beta E]$
141 respectively. Eq.4 is applicable provided the value of n is not equal to unity (1). The

142 determined end value of n, must tally with the value of E with line of best fit representing the
143 TGA data for the values of E and A to be acceptable.

144 3. Results and discussion

145 3.1. Food waste and hydrochar characterization

146 Presented in Table 1 is the moisture content of the hydrochars produced at 180, 200, and 220
147 °C. The moisture content of the hydrochar samples were in the range of 3-3.3 % which makes
148 it suitable for storage, transport, and combustion. The moisture content of the food waste
149 feedstock was found to be above this range (4.63 %). Li et al. (2019) found that the moisture
150 content of lettuce feedstock did not affect the mass yield of the HTC derived hydrochar.

151 The mass yield of the hydrochar samples produced at 180, 200 and 220 °C are
152 illustrated in Fig. 1. The HTC of the food waste produced a mass yield of 69.46% at 180 °C,
153 and thereafter decreased slightly to 68.5 % at 200 °C. Further, the increase in temperature to
154 220 °C showed a significant decrease in mass yield to 65.35 %. The reduction in mass yield
155 was due to the release of volatile matter in addition to the consecutive hydrolysis and
156 decarboxylation reaction taking place during hydrochar development (Sharma and Dubey,
157 2020). 15 % mass yield of formulated (Saqib et al., 2018) and real complex (Sharma et al.,
158 2021) food waste derived hydrochars was produced under similar conditions at 220-260 °C
159 HTC range of temperature. However, the mass yield of the hydrochars developed by HTC of
160 apple waste from 180 to 230 °C were ranged between 53 and 73% (Suárez et al., 2020).
161 Generally, high temperature leads to the decomposition of hydrochar into liquid and gaseous
162 products (Sharma and Dubey, 2020).

163 Comparing the elemental composition of the food waste mixture and hydrochars in
164 Table 1, it would be observed that food waste carbonization progressed and led to an increase
165 in the elemental carbon composition from 46.2 to 57.9% at 180 °C reaction temperature. It
166 would be further observed a slight increase carbon content of 3.2 and 0.72% was obtained

167 with a rise in temperature from 180 to 200 °C and then 200 to 220 °C, respectively. Previous
168 study under similar experimental conditions showed the respective elemental carbon content
169 of 46.70 and 61.97% for real food waste and the derived hydrochar (Akarsu et al., 2019).^[22] The
170 slight difference noticed might be due to the difference in composition, formulation, and the
171 origin of food waste feedstock.^[0]

172 The oxygen content of the food waste and hydrochars were 35.82 and 30.7-31.7%,
173 respectively.^[55] The decrease in the oxygen content of the food waste after HTC process
174 suggests the elimination of elemental oxygen through dehydration and decarboxylation. The
175 magnitude of elemental oxygen from food waste obtained during current study was lower
176 than the magnitude (45.9%) observed by Suarez et al (2020) for discarded apple residue.
177 Also, the elemental oxygen was also less than 37-54 % obtained in the works of Akarsu et al
178 (2019) and Sharma et al (2021) on municipal food waste.

179 The nitrogen and hydrogen elemental content presented in Table 1, shows significant
180 variation between the food waste and the derived carbonized hydrochar.^[0] As the HTC
181 progressed, the nitrogen content in the food waste significantly increased from 3.8 to 4.8 % at
182 180 °C, while the HTC experiments respectively conducted at 200 and 220 °C increased the
183 elemental nitrogen content to 4.9 and 5.0 %. This suggests the fact that de-amination of the
184 polysaccharide-rich date palm components present in food waste to yield ammonia did not
185 occur during the hydrochar formation process (Motavaf and Savage, 2021).^[34] In addition, the
186 observed increase in nitrogen content might be to the fact that it remains intact during oxygen
187 content loss. Saqib et al. (2018) however observed that the nitrogen content of prepared food
188 waste (5.7 %) was higher compared to the hydrochar (4.35 %) produced at temperatures up to
189 200 °C.

190 The sulphur content for both food waste and derived hydrochar was about 0.3% lesser
191 than the contents obtained during the current study for both hydrochars and food waste

192 (Table 1). The relatively higher sulphur content may be a contribution from the egg
193 component in the food waste. After combustion, nitrogen and sulphur from solid fuel creates
194 acid that causes corrosive wear on the metal surfaces of an engine.^[0]

195 Table 1 also presents the proximate analysis of the food waste and hydrochars which
196 reveals the extent of the HTC.^[0] After the HTC of the food waste at 180 °C, an expected
197 increase in fixed carbon (FC) and ash content (A) from 17.57 to 37.35% and 6.47 to 7.50%
198 was observed, respectively. This led to a corresponding decrease in volatile matter (VM)
199 from 71.33 to 51.78%.^[0] Subsequent variation in the HTC temperature of the food waste at 200
200 and 220 °C produced hydrochars with FC, A, and VM in the range of 30.81 - 36.88 %, 9.1 -
201 10.70 %, and 50.89 - 55.48 %, respectively.^[45] The ratio of the FC and VM which expresses the
202 fuel ratio of all samples was found to be less than 0.8. This value is within the range of 0.44
203 to 1.10 specified by Sharma et al. (2021) and Sharma and Dubey (2020) for hydrochars that
204 could be exploited as fuels and co-fuels in combustion systems or power plants. However, the
205 ash content (7.50-10.70%) of the hydrochars was high compared to the food waste precursor
206 (6.47 %) and may lead to slagging and fouling in the boiler when used as fuel.

207 Another important characteristic of fuel is the HHV which is also presented for the
208 prepared food waste and HTC derived hydrochar samples in Table 1. The HHV for the
209 prepared food waste was 18.17 MJ/kg, which is closer to 18.7 and 18.3 MJ/kg obtained for
210 apple (Suárez et al., 2020) and municipal (Akarsu et al., 2019) food waste, respectively.^[24] As
211 the HTC temperature was increased from 180 to 200 °C and then to 220 °C, there was a total
212 increment of 1.59% from 23.23 to 23.61%. This increment is low when compared to the
213 study on apple waste mentioned earlier where a HHV increment of 25.3% from 23.7 to 29.7
214 % was recorded.^[20] This may be due to the relatively higher temperature (230 °C) and longer
215 dwelling time (240 min) used during the study.

216 Energy yields of the produced hydrochars were determined according to Eq. 2 and
217 were used to determine the preserved densification ratio defined as Eq. 3 and listed in Table
218 1. The trend already observed for fixed carbon was similarly followed for the energy yield
219 which decreased from 88.91 to 84.30% as the HTC temperature increased. Similar trend was
220 observed by Saqib et al. (2018), where the energy yield decreased from 12.81 to 10.92%.^[2]▶
221 Yet, it would be clearly observed that both the decreased extent of energy yield and the
222 energy yield of the hydrochar obtained in this study was higher.^[31]▶ While the decreased extent
223 of the energy yield could be as a result of the longer residence time (2h) used, the relatively
224 very high energy yield obtained, may be due to the palm date component of the food waste
225 feedstock. Depending on the variety, date palm has an approximate gross energy ranging
226 between 3523.3 – 4251.5 kcal/kg (Chandrasekaran et al., 2013) which is 81.1 - 97.9% of the
227 net calorific value of the food waste mixture used in this study. It is therefore quite likely that
228 palm dates may contain larger number of high energy C-C bonds and smaller amounts of
229 lower energy H-C and O-C bonds, thus resulting to overall high energy yield.^[96]▶

230 The variation in densification ratio and energy yield of hydrochar with HTC
231 temperature are presented in Table 1. The observed energy densification ratio for hydrochar
232 was ~1.28^[26]▶ and close to the value of 1.38 obtained for municipal food wastes (Akarsu et al.,
233 2019).^[21]▶ Energy densification through HTC increases the amount of energy stored in food
234 waste in order to improve its energetic properties.^[4]▶ The energy yield of food waste and the
235 energy densification ratio of hydrochar largely depend on the bulk density and chemical
236 composition of the food waste.^[45]▶ These parameters must be determined if a hydrochar derived
237 from a food waste feedstock is to be used as fuel. Energy densification of food waste using
238 HTC processes increases hydrochar energy density for more efficient transport.^[2]▶ In summary,
239 it is clear from Table 1 that as both the mass and energy yield of the hydrochar decreased

240 both the energy densification ratio and HHV increased. Thus, the HTC220 had the highest
241 heating value (23.61 MJ/kg), while food waste had the least (18.17 MJ/kg).

242 Fig. 2 is the Van Krevelen diagram where the oxygen-carbon (O/C) and hydrogen-
243 carbon (H/C) ratios of the food waste and hydrochars were plotted. It can be seen clearly that
244 both H/C (0.39) and O/C (0.6) ratios of the hydrochars were low compared to the ratios
245 obtained for raw food waste. These ratios were lowest for HTC220 and this accounted for the
246 close proximity of HTC220 to the region representing lignite on the diagram. This implies
247 that HTC of the food waste leads to a gradual upgradation into the lignite rank.^[2] Thus, both
248 reductions in the H/C and O/C with increase in HTC temperature may be the occurrence of
249 dehydration and decarboxylation (Śliz and Wilk, 2020). This result is similar to the finding
250 of Saqib et al.^[1] (2018) where there was a steady reduction of the H/C and O/C ratios from
251 0.115 to 0.096 and 0.39 to 0.23 as the HTC temperature was elevated from 200 to 300 °C,
252 respectively.^[2]

253 Reduction in H/C and O/C ratios may be due to the decarboxylation reaction that took
254 place during the carbonization process (Sevilla et al., 2011).^[2] According to HTC process at
255 elevated temperatures which advances with dehydration reactions thereby eliminating oxygen
256 from the initial raw biomass structure, giving rise to a decrease in the O/C ratio (Maniscalco
257 et al., 2020).^[15] On the other hand, decarboxylation during HTC removes carboxyl and carbonyl
258 groups, thus, leading to a drop in O/C and H/C ratio of the food waste mixture (Smith et al.,
259 2016).^[0]

260 This work further studied the variation of physical property of food waste and
261 hydrochar samples in terms of their appearance and texture. Fig. 3, inset shows the colour
262 variation of raw food waste at different HTC temperatures. It was observed that at higher
263 temperature, the food waste (Fig. 3a, inset) changes from dark brown colour to brownish-

264 black hydrochars (Fig. 3 b–d, inset). The dried hydrochar retained its dense consistency and
265 lustreless appearance which indicates a mild coalification of the food waste to lignite.

266 A detailed SEM analysis of the food waste and hydrochars reveal insightful
267 information on change of the structural morphology of the food waste during HTC (Fig. 3).
268 The magnified SEM images show slight changes in the surface structure of food waste and
269 the hydrochars due to lignin loss arising from degradation and depolymerisation reactions
270 taking place during the hydrochar formation process. Microscopic examination of food waste
271 presented a surface structure that was densely packed, impervious, and fixed. After HTC, the
272 surface structures of HTC180 and HTC200 were altered which may be consequence of the
273 collapse of chemical structures of the cellulose and lignin content in the food waste. The
274 sheet, debris and crack-like surface structure detected on the SEM image of HTC220, may be
275 due to further volatile releases and elimination of the hydroxyl, ketone, and aldehyde
276 functional groups present in the carbohydrate constituent of the food waste. Sheet, debris and
277 crack-like surface structures were similarly observed on the SEM images of lignite in the
278 investigation carried out by Tang et al. (2016).

279 Different food wastes have been found to have distinct surface structure under varied
280 operating conditions (Saqib et al.,^[13] 2018) and some of these differences in surface structure for
281 different food wastes are reported in the literature. A three-component food waste with high
282 carbohydrate content was hydrothermally carbonized at 200 °C for 6 hr. The microstructural
283 analysis of the surface of the derived hydrochar revealed a carbon microsphere (Tradler et al.,
284 2018). Another food waste with high carbohydrate content was hydrothermally carbonized at
285 220 °C for 1 h. The flakey-like microstructure of the food waste was metamorphosed to a
286 hydrochar with carbon spheres and microsphere-like microstructure after HTC. The surface
287 structure metamorphosis was imaginably due to condensation of the soluble product and
288 consecutive polymerization reaction (Sharma and Dubey, 2020). Steamed bread was also

289 hydrothermally carbonized at 260 °C and reaction time of 3 h into a hydrochar. Trace
290 quantities of sphere-like particles were noticed on its microstructure which was imaginably
291 due to carbonization of its constituent starch (Feng et al., 2019).^[22]▶

292 FT-IR analysis was carried on the food waste and hydrochar samples in order to
293 ascertain the functional groups that may be present on their respective surface (Fig. 4). The
294 FT-IR spectra showed a disappearance and shift of some absorption bands. A broad band
295 located on the FT-IR spectrum range of 3200 - 3400 cm⁻¹ may be assigned to the hydroxyl
296 group functional group.^[0]▶ For both the raw food waste and hydrochar samples, absorption band
297 at frequencies between 2852 and 2921 cm⁻¹ were due to the presence of C-H stretch of
298 aliphatic methylene group. These absorption bands may be evidence of contributions from
299 spent coffee and palm dates contained in the food waste mixture.^[63]▶ The bands around 1700 to
300 1740 cm⁻¹ in the raw food waste sample can be attributed to the C=O stretch of aldehydes
301 usually contained in palm dates (Bharath et al., 2020). The disappearance of C=O bands after
302 HTC reveals that the carboxylic groups present in palm dates component of the food waste
303 mixture might have been converted to carbon dioxide and polysaccharide pieces (Robbiani,
304 2013). The disappearance of the C-H band implies that the aliphatic structure of the food
305 waste was not preserved during HTC.

306 The peak located at 1630 cm⁻¹ in raw food sample was widely accepted to be due
307 to water. This peak shifted to a lower frequency at 1602 and 1607 cm⁻¹ after HTC process.^[31]▶
308 The aromatic ring related vibrations between 1500 and 1600 cm⁻¹ may be due to the presence
309 of C=C stretch. The aromatic ring -related vibrations of C=C stretch suggests that Maillard
310 reaction between the carbohydrate and egg components in the food waste led to an increased
311 aromatisation of transient species. This reaction could have been responsible for the increase
312 in the atomic nitrogen in the hydrochar samples obtained from the elemental test analysis.

313 The presence of band at $\sim 1455 \text{ cm}^{-1}$ was good evidence for $=\text{CH}_2$ stretch of
314 methylene, while the band around 1376 cm^{-1} was associated with $-\text{CH}_3$ bend (methyl). The
315 presence of absorption bands between 1240 and 1070 cm^{-1} suggests the presence of C-O-C
316 stretching of esters. The vibration from 1200 to 900 cm^{-1} in both the raw food waste and
317 hydrochar samples shows the presence of C-O-C linkage present in bread and other baked
318 biomass.

319 3.2. Combustion behaviour and kinetics

320 The thermogravimetric analysis was applied to study the food waste combustion behaviour
321 and Fig. 5a presents the plot of TG and DTG versus temperature for feedstock waste.
322 Evidently, the combustion of the food waste started from 59 - $159 \text{ }^\circ\text{C}$ where a $4.6 \text{ wt. } \%$ weight
323 loss was recorded within the temperature range. The recorded weight loss may be due water
324 evaporation. The combustion of the feedstock advanced in distinct stages as seen in the DTG
325 curves. The DTG curve for food waste reveals three peaks within a temperature ranging from
326 50 to $383 \text{ }^\circ\text{C}$. The maximum weight loss rate recorded within this temperature range was 4.6
327 $\%/\text{min}$ which corresponds to $47.2 \text{ } \%$ weight loss. At $750 \text{ }^\circ\text{C}$, where there was complete
328 conversion of food waste to elemental carbon, $6.68 \text{ } \%$ solid residue in the form of ash was
329 left.

330 The combustion of mixture of the food waste observed by the DTG result showed a
331 three-peak combustion process. The food waste mixture may be characterized as fruity (tea
332 leaves and banana peels), woody (palm dates and spent coffee) and edible (bread and egg)
333 biomass. Thus, these ingredients present in the food waste contain different amounts of
334 hemicellulose, cellulose, and lignin.^{[0]▶}

335 The first peak of food waste combustion at $106 \text{ }^\circ\text{C}$ is believed to be the effect of water
336 evaporation of the food waste mixture or combustion of the high volatile content white bread
337 and egg component of the food waste. The second combustion peak at $201 \text{ }^\circ\text{C}$ is imagined to

338 be the effect of combustion of the bread and egg volatiles and banana peel/spent tea leaves
339 biomass char. The third combustion peak of the food waste at 293 °C is linked with the
340 combustion of palm dates and spent coffee char.^[1] The observed maximum rates of mass loss
341 occurring at higher temperatures in peak 3 was attributed to combustion of palm dates and
342 spent coffee because of its woody nature or relatively high lignin content.

343 For HTC220 sample, the TG and DTG versus temperature plot, displayed in Fig. 5b
344 showed significant variation in weight loss. As seen in the DTG plot, the peak temperatures
345 for the HTC220 were 84.4 and 330 °C for peaks 1 and 2, respectively. In a similar work
346 carried out on lignite samples (Mo et al., 2020) observed peak at 95 °C and other peak was
347 located between 105 and 350 °C on TG curves. The first and second peaks were attributed to
348 the occurrence of water evaporation and simultaneous oxidation/devolatilization reaction
349 respectively. It was noted that the number of DTG peaks for raw food waste reduced from 3
350 to 2 after HTC. The observed reduction of DTG peaks after HTC-220 may be due to
351 diminished volatile matter content, degraded lignin structures and enhanced fixed carbon
352 content of the hydrochar.^[1] The second DTG peak of HTC220 was very broad (indicating a
353 gradual combustion reaction of the char) compared to the sharp nature of the first peak which
354 reveals the occurrence of a rapid or flash combustion process.

355 The TG plot of the hydrochar (Fig.5b) showed the highest drop in weight of 53.9 wt.
356 % within the temperature range of 330-670 °C. The initial degradation temperature for the
357 HTC was around 96.4 °C, but it was delayed for feedstock from 154 to about 250 °C.^[23] This
358 could be due to the higher proportion of moisture contained in the food waste was relative to
359 the hydrochar. The combustion of HTC220 can be described as a two-stage process based on
360 the peak identified on the DTG plot. The first stage of combustion of HTC220 was observed
361 in the 50-170 °C temperature range, while the second stage of the combustion stage was
362 noticed between 170 and 700 °C temperature.

363 The activation energies for food waste feedstock and hydrochars corresponding to
364 each peak earlier detected are listed in Table 2. The activation energy of the feedstock was
365 found to be in range of 29.98 to 33.51 kJ/mol. Judging from the kinetic plots (Fig. 6), the
366 Arrhenius equation model reasonably describes the combustion reaction of both food waste
367 feedstock and hydrochars. The respective activation energies of the feedstock were 33.51,
368 24.02, and 29.98 kJ/mol for peaks 1, 2, and 3. The fluctuating trend of the activation energy
369 across the three peaks indicate that the combustion of food waste and hydrochars occurring at
370 different stages involve different mechanism.

371 Two peaks were noticed for the hydrochar and the respective activation energies
372 calculated for the first and second peaks were 25.47 and 16.52 kJ/mol. The reduction in
373 activation was observed by Saqib et al. (2018) where the activation energy of the hydrochars
374 prepared under similar conditions were reduced from 56.78 to 47.38 kJ/mol from first peak to
375 second peak. ^[23] This reduction in activation energy in both feedstock and hydrochar sample may
376 be attributed to the catalytic effect of inorganic species present in the hydrochar (Smith et al.,
377 2016). However, in another related study on combustion of lignite samples, the activation
378 energy of hydrochar increased 59.95 to 69.49 kJ/mol with increase in HTC temperature from
379 270 to 330°C (Mo et al., 2020).

380 It can be inferred in Table 2 that HC220 showed an early liberation of energy in
381 contrast to raw food waste during combustion with activation energy of 25.47 kJ/mol and
382 16.52 kJ/mol in contrast to 33.51 kJ/mol and 24.02 kJ/mol for feedstock in peaks 1 and 2,
383 respectively. This indicates that the hydrochar may be mixed with low rank in order to reduce
384 its ignition temperature. Similar view was asserted by Gupta et al. ^[2] (2020) based on an
385 outcome of an investigation which revealed that the activation energy of the real food waste
386 was 82 kJ higher than the derived hydrochar at 200 °C.

387 4. Conclusions

388 Hydrochars produced from simulated food waste (similar to Hajj and Umrah food waste)
389 through HTC process route has been carried out.^[0] The results showed that with increase in
390 temperature, the mass and energy yields of the hydrochars decreased, while the energy
391 densification ratio and HHV of hydrochars increased. Furthermore, the hydrochar produced
392 at 220 °C had the HVV of 23.61 MJ/kg, which was a significant improvement compared to
393 the HHV of 18.17 MJ/kg, obtained for food waste precursor. The combustion kinetic showed
394 that the energy required to start the combustion reaction for hydrochar (25.47 kJ/mol) was
395 lower compared to the energy (33.51 kJ/mol) required for a reaction with raw food waste.
396 Hence, the results conclude that the reported strategy could be an effective alternate to
397 convert Hajj and Umrah food waste to a value-added solid fuel.

398 Acknowledgement

399 This project was funded by the National Plan for Science, Technology and Innovation
400 (MAARIFAH), King Abdulaziz City for Science and Technology, Kingdom of Saudi Arabia
401 (Award Number 14-ENV665-02).

402 References

403 Abdullah, R.F., Rashid, U., Ibrahim, M.L., Hazmi, B., Alharthi, F.A., Nehdi, I.A., 2020.

404 Bifunctional nano-catalyst produced from palm kernel shell via hydrothermal-assisted
405 carbonization for biodiesel production from waste cooking oil. *Renew. Sustain. Energy*
406 *Rev.* 137, 110638. doi: 10.1016/j.rser.2020.110638.

407 Akarsu, K., Duman, G., Yilmazer, A., Keskin, T., Azbar, N., Yanik, J. 2019. Sustainable
408 valorization of food wastes into solid fuel by hydrothermal carbonization. *Biores.*
409 *Technol.* 292, 121959. doi: 10.1016/j.biortech.2019.121959.

410 Alibardi, L., Cossu, R., 2016. Effects of carbohydrate, protein and lipid content of organic
411 waste on hydrogen production and fermentation products. *Waste Manag.* 47, 69–77.
412 doi: 10.1016/j.wasman.2015.07.049.

413 Al-Aboosi, F.Y., El-Halwagi, M.M., Moore, M., Nielsen, R.B., 2021. Renewable ammonia as
414 an alternative fuel for the shipping industry. *Curr. Opin. Chem. Eng.* 31, 100670.
415 <https://doi.org/10.1016/j.coche.2021.100670>

416 Alshareef, S.A., Alqadami, A.A., Khan, M.A., Alanazi, H.S., Siddiqui, M.R., Jeon, B-H.,
417 2022. Simultaneous Co-hydrothermal Carbonization and Chemical Activation of Food
418 Wastes to Develop Hydrochar for Aquatic Environmental Remediation. *Biores. Technol.*
419 347, 126363. doi: 10.1016/j.biortech.2021.126363

420 Alshareef, S.A., Otero, M., Alanazi, H.S., Siddiqui, M.R., Khan, M.A., Alothman, Z.A. 2021.
421 Upcycling olive oil cake through wet torrefaction to produce hydrochar for water
422 decontamination. *Chem. Eng. Res. Design* 170, 13 – 22.

423 Atique, S., Itumalla, R., 2020. Hajj in the time of COVID-19. *Infect Dis. Heal.* 25(3), 219–
424 221. doi: 10.1016/j.idh.2020.04.001.

425 Baig, M.B., Gorski, I., Neff, R.A., 2019. Understanding and addressing waste of food in the
426 Kingdom of Saudi Arabia. *Saudi J. Biol. Sci.* 26(7), 1633–1648. doi:
427 10.1016/j.sjbs.2018.08.030.

428 Bharath, G., Hai, A., Rambabu, K., Banat, F., Jayaraman, R., Taher, H., Bastidas-Oyanedel,
429 J.R., Ashraf, M.T., Schmidt, J.E., 2020. Systematic production and characterization of
430 pyrolysis-oil from date tree wastes for bio-fuel applications. *Biomass and Bioenergy*
431 135, 105523. <https://doi.org/10.1016/j.biombioe.2020.105523>

432 Cao, J., Gao, Y., Ma, Y., 2019. Facile preparation of activated carbon foam via pyrolysis of
433 waste bread under CO₂ atmosphere. *Biomass Conv. Bioref.* 9, 521–529. doi:
434 10.1007/S13399-019-00437-X.

435 Carmona-Cabello, M., García, I.L., Papadaki, A., Tsouko, E., Koutinas, A., Dorado, M.P.,
436 2020. Biodiesel production using microbial lipids derived from food waste discarded
437 by catering services. *Biores. Technol.* 323, 124597. doi:

438 10.1016/j.biortech.2020.124597.

439 Chandrasekaran, M., Bahkali, A.H. 2013. Valorization of date palm (*Phoenix dactylifera*)
440 fruit processing by-products and wastes using bioprocess technology – Review. Saudi
441 J. Biol. Sci. 20(2), 105–120. doi: 10.1016/j.sjbs.2012.12.004.

442 Feng, Y., Sun, H., Han, L., Xue, L., Chen, Y., Yang, L., Xing, B. 2019. Fabrication of
443 hydrochar based on food waste (FWHTC) and its application in aqueous solution rare
444 earth ions adsorptive removal: Process, mechanisms and disposal methodology. J.
445 Clean. Prod. 212, 1423–1433. doi: 10.1016/j.jclepro.2018.12.094.

446 Gupta, D., Mahajani, S.M., Garg, A., 2020. Investigation on hydrochar and macromolecules
447 recovery opportunities from food waste after hydrothermal carbonization. Sci. Total
448 Environ. 749, 142294. doi: 10.1016/j.scitotenv.2020.142294.

449 Ishangulyyev, R., Kim, S., Lee, S.H., 2019. Understanding food loss and waste-why are we
450 losing and wasting food? Foods 8(8), 297. doi: 10.3390/foods8080297.

451 Li, L., Diederick, R., Flora, J.R.V., Berge, N.D., 2013. Hydrothermal carbonization of food
452 waste and associated packaging materials for energy source generation. Waste Manag.
453 <https://doi.org/10.1016/j.wasman.2013.05.025>

454 Li, Y., Liu, H., Xiao, K., Hu, H., Li, X., Yao, H., 2019. Correlations between the
455 physicochemical properties of hydrochar and specific components of waste lettuce:
456 Influence of moisture, carbohydrates, proteins and lipids. Biores. Technol. 272, 482–
457 488. doi: 10.1016/j.biortech.2018.10.066.

458 Maniscalco, M.P., Volpe, M., Messineo, A. 2020. Hydrothermal carbonization as a valuable
459 tool for energy and environmental applications: A review. Energies 13(16), 4098. doi:
460 10.3390/en13164098.

461 Motavaf, B., Savage, P.E., 2021. Effect of process variables on food waste valorization via
462 hydrothermal liquefaction . ACS EST Engg. 1(3), 363–374. doi:

463 10.1021/acsestengg.0c00115.

464 Mo, Q., Liao, J., Chang, L., Han, Y., Chaffee, A.L., Bao, W., 2020. Study on combustion
465 performance of hydrothermally dewatered lignite by thermal analysis technique. *Fuel*
466 285, 119217. doi: 10.1016/j.fuel.2020.119217.

467 Nizami, A.S., Shahzad, K., Rehan, M., Ouda, O.K.M., Khan, M.Z., Ismail, I.M.I., Almeelbi,
468 T., Basahi, J.M., Demirbas, A., 2017. Developing waste biorefinery in Makkah: A way
469 forward to convert urban waste into renewable energy. *Appl. Energy* 186, 189–196.
470 <https://doi.org/10.1016/j.apenergy.2016.04.116>

471 Robbiani, Z., 2013. Hydrothermal carbonization of biowaste / fecal sludge: Conception and
472 construction of a HTC prototype research unit for developing countries. Master Thesis,
473 April, p. 88.

474 Sait, H.H., Hussain, A., Salema, A.A., Ani, F.N., 2012. Pyrolysis and combustion kinetics of
475 date palm biomass using thermogravimetric analysis. *Biores. Technol.* 118, 382–389.
476 doi: 10.1016/j.biortech.2012.04.081.

477 Saqib, N.U., Baroutian, S., Sarmah, A.K., 2018. Physicochemical, structural and combustion
478 characterization of food waste hydrochar obtained by hydrothermal carbonization.
479 *Biores. Technol.* 266, 357–363. doi: 10.1016/j.biortech.2018.06.112.

480 Sevilla, M., Maciá-Agulló, J.A., Fuertes, A.B., 2011. Hydrothermal carbonization of
481 biomass as a route for the sequestration of CO₂: Chemical and structural properties of
482 the carbonized products. *Biomass Bioenergy* 35(7), 3152–3159. doi:
483 10.1016/j.biombioe.2011.04.032.

484 Sharma, H.B., Dubey, B.K., 2020. Co-hydrothermal carbonization of food waste with yard
485 waste for solid biofuel production: Hydrochar characterization and its pelletization.
486 *Waste Manag.* 118, 521 – 533. doi: 10.1016/j.wasman.2020.09.009.

487 Sharma, H.B., Panigrahi, S., Dubey, B.K., 2021. Food waste hydrothermal carbonization:

488 Study on the effects of reaction severities, pelletization and framework development
489 using approaches of the circular economy. *Biores. Technol.* 333, 125187. doi:
490 10.1016/j.biortech.2021.125187.

491 Singh, D., Yadav, S., 2019. Evaluation of the physico-chemical development of kitchen food
492 wastes through torrefaction - a biodiversity case study. *Biomass Conv. Bioref.* 11,
493 1353–1362. doi: 10.1007/S13399-019-00526-X.

494 Śliz, M., Wilk, M. A., 2020. Comprehensive investigation of hydrothermal carbonization:
495 Energy potential of hydrochar derived from Virginia mallow. *Renew. Energy* 156,
496 942–950. doi: 10.1016/j.renene.2020.04.124.

497 Smith, A.M., Singh, S., Ross, A.B., 2016. Fate of inorganic material during hydrothermal
498 carbonisation of biomass: Influence of feedstock on combustion behaviour of
499 hydrochar. *Fuel* 169, 135–145. doi: 10.1016/j.fuel.2015.12.006.

500 Suárez, L., Benavente-Ferraces, I., Plaza, C., de Pascual-Teresa, S., Suárez-Ruiz, I., Centeno,
501 T.A. 2020. Hydrothermal carbonization as a sustainable strategy for integral
502 valorisation of apple waste. *Biores. Technol.* 309, 123395, doi:
503 10.1016/j.biortech.2020.123395.

504 Tang, J., Feng, L., Li, Y., Liu, J., Liu, X., 2016. Fractal and pore structure analysis of Shengli
505 lignite during drying process. *Powder Technol.* 303, 251–259. doi:
506 10.1016/j.powtec.2016.09.042.

507 Tradler, S.B., Mayr, S., Himmelsbach, M., Priewasser, R., Baumgartner, W., Stadler, A.T.,
508 2018. Hydrothermal carbonization as an all-inclusive process for food-waste
509 conversion. *Biores. Technol. Reports* 2, 77–83. doi: 10.1016/j.biteb.2018.04.009.

510 “UNEP Food Waste Index Report 2021 | UNEP - UN Environment Programme.”
511 <https://www.unep.org/resources/report/unep-food-waste-index-report-2021> (accessed
512 Mar. 06, 2021).

513 Yan, M., Liu, Y., Song, Y., Xu, A., Zhu, G., Jiang, J., Hantoko, D., 2022. Comprehensive
514 experimental study on energy conversion of household kitchen waste via integrated
515 hydrothermal carbonization and supercritical water gasification. Energy 242, 123054.
516 <https://doi.org/10.1016/j.energy.2021.123054>

517

518

519

520

521

522

523

524

525

526

527

528

529

530

531

532

533

534

535

536

537